

Highlights

Reducing RES Droughts through the integration of wind and solar PV

Boris Morin, Aina Maimó Far, Damian Flynn, Conor Sweeney

- RES droughts are analysed using 45 years of hourly wind and solar PV generation data
- RES droughts from C3S-Energy and ERA5-Atlite datasets are compared
- Adding solar PV to a wind-dominated system reduces RES drought frequency and duration
- Validated RES datasets are crucial to accurately identify RES drought extremes

Reducing RES Droughts through the integration of wind and solar PV

Boris Morin^{a,*}, Aina Maimó Far^a, Damian Flynn^b, Conor Sweeney^a

*^aSchool of Mathematics and Statistics, University College Dublin, Belfield, Dublin
4, Dublin, D04 V1W8, Ireland*

*^bSchool of Electrical and Electronic Engineering, University College Dublin, Belfield,
Dublin 4, Dublin, D04 V1W8, Ireland*

*Corresponding author

Email addresses: `boris.morin@ucdconnect.ie` (Boris Morin),
`aina.maimofar@ucd.ie` (Aina Maimó Far), `damian.flynn@ucd.ie` (Damian Flynn),
`conor.sweeney@ucd.ie` (Conor Sweeney)

Abstract

Increasing the share of electricity produced from renewable energy sources (RES), combined with RES dependence on weather, poses a critical challenge for energy systems. This study investigates the importance of the balance between wind and solar photovoltaic (PV) capacity on periods of low renewable generation, known as RES droughts. Three different RES datasets are used to estimate the capacity factors for different scenarios of installed capacities for wind and solar PV power. The skill of the RES models is quantified by comparing capacity factor time series to observed hourly data and by assessing their representation of observed RES droughts. The RES models are used to generate a 45-year hourly time series of RES capacity factor, enabling analysis of the frequency, duration and return periods of RES droughts at a climatological scale. Results show the importance of using an accurate, validated RES model for RES drought risk assessment. The addition of solar PV capacity to a wind-dominated system results in a significant reduction in the frequency and duration of RES droughts, while also reducing extremes and seasonal RES drought patterns. These findings underscore the importance of diversification in RES capacity to enhance energy security and resilience.

Keywords: RES Drought, Wind Power, Solar PV Power, Renewable Energy Sources, Return Periods

1. Introduction

The EU aims to generate at least 69% of its electricity from renewable energy sources (RES) by 2030, up from 41% in 2022 [1]. While this transition is essential for reducing greenhouse gas emissions, it also highlights the challenge of managing the variability of weather-dependent energy sources such as wind and solar photovoltaic (PV) power. This challenge is amplified by the increasing electrification of energy sectors, which places greater demand on the power system and makes it more sensitive to meteorological conditions, both in historical [2] and future climates [3]. Periods of low renewable generation, known as *Dunkelflaute* or RES droughts, pose significant risks to system adequacy and energy security, emphasising the need for a resilient energy system to meet both growing electricity demand and decarbonisation targets.

RES drought events do not have a fixed definition, with various approaches present in the literature. One common method defines a RES drought as a period during which the average capacity factor (CF) remains below a fixed threshold for a specified duration. For example, Kaspar et al. [4] used this method to investigate the shortfall risks of low wind and solar PV generation in Europe, with a focus on Germany, testing multiple CF thresholds and durations. Similarly, Mockert et al. [5] examined the link between weather regimes and RES droughts in Germany using a 48-hour rolling window under a threshold to define RES droughts. Similar fixed-threshold approaches have also been applied using CF series reconstructed through machine learning in regions such as Japan [6] and Hungary [7].

Alternative methods adjust the CF threshold dynamically over the year to account for seasonal variations in renewable production. Raynaud et al. [8] defined RES droughts as sequences of days with renewable electricity generation below a threshold that varies seasonally, a methodology later adapted for India [9]. Building on this, Kapica et al. [10] compared the likelihood of increased RES droughts in Europe under different climate models. Other studies have defined RES droughts based on deviations from daily mean production: Rinaldi et al. [11] applied these in the U.S. Western Interconnection to quantify the benefits of long-term storage, while Brown et al. [12] examined weekly timescales to explore meteorological influences on the most severe RES drought events. Another method defines RES drought indices based on metrics commonly used in hydro-meteorology to characterise RES droughts [13]. This index was also applied to the U.S. by Bracken et al. [14], revealing a consistent increase in the RES drought magnitude when load is considered, despite showing differing results across regions. The consideration of demand introduces a completely different factor to generation: weather is not the only driver, as the societal component plays a large role.

In addition to examining periods of low renewable electricity generation, several studies also explore the periods when the imbalance between renewable generation and electricity demand (residual load) is high. Raynaud et al. [8] defined both energy production and energy supply droughts, and showed the difference in their patterns in a hypothetical fully renewable system composed of wind, PV and run-of-the-river hydropower. Similarly, Allen and Otero [13] also defined a standardised index based on meteorological droughts to address residual load, whose correlation to the energy production index is mostly negative (as expected, although quite low anticorrelations and even small positive correlations appear for some European countries). This

index was also applied to the U.S. by Bracken et al [14], revealing a consistent increase in the drought magnitude when load is considered, despite showing differing results across regions.

In this paper, the focus is exclusively on renewable electricity generation, which allows us to maintain physical models that do not consider the behavioural influence of demand, whose role will be addressed in the discussion. A fixed threshold approach is used to define RES droughts, which facilitates consistent inter-comparison between scenarios with different installed wind and solar PV capacities. The case study used in this paper is Ireland, a region with a strong reliance on wind power and ambitious targets for solar PV power expansion. This provides valuable insights into the potential benefits of diversifying the renewable energy mix on RES droughts in the context of realistic scenarios.

RES droughts are identified using onshore wind and solar PV CF time series. In this study, three different datasets are used and compared, all of which are driven by the ERA5 reanalysis [16]. Two of the datasets are part of C3S Energy (C3SE), an energy-based operational dataset produced by the EU Copernicus Climate Change Service [17]. One of the C3SE datasets provides CF time series aggregated at the national scale, while the other provides the CF time series at each grid point, at the ERA5 resolution of 0.25° . The third dataset was generated using the Atlite model [18], which converts the ERA5 atmospheric data to a generation time series using specified wind turbine and PV panel models. Atlite is an open-source tool developed by PyPSA [18] and has been used for estimating wind and solar PV generation in order to study RES droughts [5].

Generic datasets for wind and solar PV CF are often used for the quantification of RES droughts. Despite undergoing a validation process, they are often not fully representative of each geographical location, and can show differences in the number of RES drought events [19]. In this work, we quantify the skill of a dataset developed for the European region (C3SE), when used for a specific country (Ireland). In particular, we investigate the impact of a generic versus a tailored dataset on the analysis of RES droughts, in the context of a transition from a wind-dominated system to one with a larger share of solar PV.

The aim of this study is to answer three questions which are relevant for systems with a large share of RES generation:

- Do generic datasets have sufficient skill to reliably quantify extreme

89 RES drought events?

- 90 • What is the importance of using accurate RES farm locations, and
91 regionally-validated wind and solar PV models, when analysing of RES
92 droughts?
- 93 • How does the integration of solar PV into a predominantly wind-based
94 system alter the characteristics of RES drought events?

95 The datasets used in this study are detailed in section 2, which describes
96 their characteristics and relevance for evaluating RES droughts. Section 3
97 outlines the RES datasets used to simulate wind and solar PV generation and
98 provides the methodology for defining and identifying RES drought events,
99 including the thresholds and metrics applied. In section 4, the datasets are
100 first verified against observed energy data to assess their accuracy, followed by
101 an analysis of RES drought occurrences for two scenarios with different ratios
102 of installed wind to solar PV capacities. Finally, section 5 offers a discussion
103 of the results in the context of energy reliability and future planning, followed
104 by the main conclusions and recommendations for further research.

105 2. Data

106 This study uses publicly available datasets to construct and validate the
107 datasets for estimating the CF of wind and solar PV power. The primary
108 data sources include: EirGrid and SONI, the transmission system operators
109 (TSO) for the Republic of Ireland and Northern Ireland, respectively; the
110 ERA5 reanalysis dataset; and the C3SE dataset.

111 2.1. Wind and solar PV Capacity and Availability

112 EirGrid, the TSO for the Republic of Ireland, and SONI, the Northern
113 Ireland TSO, provide detailed datasets on all wind and solar PV farms across
114 the island of Ireland (Republic of Ireland and Northern Ireland) from 1990
115 to the present [20]. These datasets include information such as each farm’s
116 installed capacity, name, and connection date. To enhance the accuracy of
117 this data, the longitude and latitude for each farm were manually determined
118 through online searches. For simplicity, this data will be referred to as orig-
119 inating from EirGrid, as all-island data was directly obtained from EirGrid,
120 and the combined regions of the Republic of Ireland and Northern Ireland
121 will be referred to as Ireland throughout the remainder of this document.

122 The spreadsheet available from the EirGrid website contains two key vari-
123 ables: generation and availability. Generation is the energy that a RES farm
124 actually contributed to the grid, which may include limitations introduced
125 by the TSO to maintain grid stability, such as constraints and curtailment.
126 Availability represents the energy that would have been generated from a RES
127 farm if no grid constraints had been applied, making it representative of the
128 weather-related response. Generation and availability values are available
129 from 2014 onward for wind power and from 2018 onward for solar PV power,
130 although solar PV availability data only became present in the Republic of
131 Ireland in 2023. This study focuses on availability for all analyses.

132 2.2. Atmospheric Variables

133 All of the datasets used in this study are driven by data from the ERA5 re-
134 analysis [16], produced by the European Centre for Medium-Range Weather
135 Forecasts (ECMWF). This global gridded dataset provides hourly atmo-
136 spheric variables from 1940 to the present at a horizontal resolution of 0.25° .
137 Table 1 lists the relevant ERA5 variables.

Table 1: ERA5 variables used to calculate wind and solar PV generation

ERA5 name	variable
100 metre zonal and meridional wind speed	u_{100}, v_{100}
2 metre temperature	$t2m$
Surface net solar radiation	ssr
Surface solar radiation downwards	$ssrd$
Top of atmosphere incident radiation	$tisr$
Total sky direct solar radiation at surface	$fdir$

138 2.3. C3S Energy

139 The EU Copernicus Climate Change Service developed the C3S-Energy
140 (C3SE) renewable energy dataset for Europe [17], using ERA5 atmospheric
141 variables and weather-to-energy models. This dataset provides hourly CF for
142 wind and solar PV energy from 1979 to the present. The data are available
143 on the same grid as the ERA5 data, which has a horizontal resolution of
144 0.25° . The time series are also available for download at two aggregated
145 scales: regional (NUTS 2) and national.

146 The wind CF in C3SE was calculated using wind speeds at 100 metres
147 (u_{100}, v_{100}) and a standard turbine model, the Vestas V136/3450, with a fixed

148 hub height of 100 meters. As data on wind turbine fleet locations and speci-
 149 fications are difficult to obtain across Europe, C3SE assumes a homogeneous
 150 distribution of wind turbines across the ERA5 grid. While this approach
 151 does not capture the precise capacity factors reported by grid operators, it
 152 provides a well-correlated time series that effectively represents the impact
 153 of climate variability on wind power generation. The C3SE solar PV CF was
 154 also calculated for the ERA5 grid. It is derived from meteorological data, in-
 155 cluding surface solar radiation downwards (*ssrd*) and air temperature (*t2m*),
 156 using a reference solar PV plant model. This model incorporates empirical
 157 calculations for key system components such as optical losses, module effi-
 158 ciency, and inverters. The final CF accounts for a mix of module orientations
 159 typical for each location [21].

160 **3. Methods**

161 This study uses onshore wind and solar PV CF time series from three
 162 datasets to analyse RES droughts across the island of Ireland. Data down-
 163 loaded from C3SE were used to obtain two datasets: one based on national-
 164 level data (C3S NAT), and another on grid-level data (C3S GRD). The third
 165 dataset was computed using the Atlite model (ATL).

166 *3.1. C3S Energy National: C3S NAT*

167 The C3S NAT dataset is created by combining two inputs provided by
 168 C3SE at the corresponding NUTS levels: Republic of Ireland (NUTS0: IE)
 169 and Northern Ireland (NUTS2: UKN0). The two inputs are combined, using
 170 the actual installed capacity as weights. This dataset assumes that RES
 171 generation occurs at every ERA5 grid point in Ireland.

172 *3.2. C3S Energy Gridded: C3S GRD*

173 The C3S GRD dataset uses, as inputs, the actual locations of the RES
 174 farms in Ireland, and the CF from C3SE over the ERA5 grid. For each
 175 farm, the CF from the nearest grid point on the C3SE dataset was selected.
 176 A weighted average of the CF associated with each farm, using the farm's
 177 installed capacities, was used to produce the total CF time series.

178 3.3. *Atlite: ATL*

179 The ATL dataset is produced using the Atlite model. Atlite allows the
180 user to define the wind turbine power curve and PV panel model to use
181 when converting weather variables to wind and solar PV generation. The
182 Atlite model takes as inputs the locations of RES farms and ERA5 weather
183 variables: wind speed at 100 metres (u_{100} , v_{100}) for wind generation, and
184 radiation variables (ssr , $ssrd$, $tisr$, and $fdir$) along with air temperature
185 ($t2m$) for solar PV generation. The output of the Atlite model is a generation
186 time series, which is divided by the total capacity to transform it back into
187 CF. The selection of the wind turbine power curve and PV panel model
188 represents the key difference between this dataset and C3S GRD. This study
189 identifies the most appropriate wind turbine power curve to use from the
190 121 power curves, each at five different levels of smoothing, made available
191 by Renewables.ninja [22], and selects the PV panel model out of the options
192 available within Atlite.

193 3.4. *Energy Scenarios*

194 The three datasets provide CF time series for both wind and solar PV. In
195 addition to analysing the CF of wind and solar PV separately, a combined
196 CF was computed for each dataset by averaging wind and solar PV CF,
197 weighted by their installed capacities at the end of 2023 (5.9 GW for wind
198 power and 0.6 GW for solar PV power). This configuration is referred to as
199 the 91W-9PV scenario, reflecting the distribution of 91% wind and 9% solar
200 PV capacity. Given that solar PV capacity in Ireland is low in 2023, and to
201 explore how a more balanced distribution of wind and solar PV capacities
202 might impact RES droughts, this study also considered a second scenario,
203 referred to as 57W-43PV, where the installed solar PV capacity is assumed
204 to increase to 8.6 GW, while wind capacity rises to 11.45 GW. These values
205 are based on targets outlined in the roadmap published by the 2024 Climate
206 Action Plan [23]. This study does not include offshore wind in the analysis.
207 Recent reports suggest that even by 2030, Ireland is unlikely to have any
208 significant new offshore wind farms, with projected offshore capacity expected
209 to remain near zero using realistic scenarios [24].

210 New time series were generated for both the ATL and C3S GRD solar
211 PV datasets, incorporating a revised distribution of installed capacity across
212 Ireland as specified in the roadmap. For wind power, the CF time series
213 remains unchanged, as significant shifts in the location of wind farms are not
214 expected. In total, twelve CF time series were analysed in this study, six for

individual wind and solar PV CF (three datasets for each source) in the 91W-9PV scenario, and an additional six time series that include the combined CF for 91W-9PV and 57W-43PV scenarios across the different datasets.

It is important to note that the specific capacity values used in this study are illustrative and are not intended to reflect precise future realities. Instead, they serve to explore the impact of transitioning from a wind-dominated system (91W-9PV) to a more evenly distributed system (57W-43PV). This approach allows for a comparative analysis between the two scenarios, assessing how the balance of RES capacity affects the occurrence of RES droughts.

For each dataset (ATL, C3S GRD, and C3S NAT), four distinct scenarios are examined, as summarised below:

- Wind Power - based on the actual capacity at the end of 2023
- Solar PV Power - based on the actual capacity at the end of 2023
- Combined RES / 91W-9PV - based on the actual capacity at the end of 2023
- Combined RES / 57W-43PV - based on the projected capacity for 2030

3.5. RES Drought Definition

In this study, a RES drought event was defined as occurring when the 24-hour moving average of CF remains below a fixed threshold of 0.1 for a period of longer than 24 hours. By using a 24-hour moving average, fewer but longer-lasting events were captured compared to using the raw CF time series, which can be more sensitive to short-term fluctuations. The 24-hour rolling average also avoids potential masking of day-long events due to their start time. A fixed threshold approach was chosen in this study to enable consistent inter-comparison between datasets.

The moving average approach smooths out short-term fluctuations, so that brief periods above the threshold do not interrupt an otherwise continuous low-CF period (Fig. 1). This means that a single hour above the threshold does not "break" a RES drought event if it is surrounded by prolonged low-generation hours. As a result, fewer but longer-lasting RES drought events are identified, which may better reflect real-world conditions where energy supply constraints persist over extended periods.

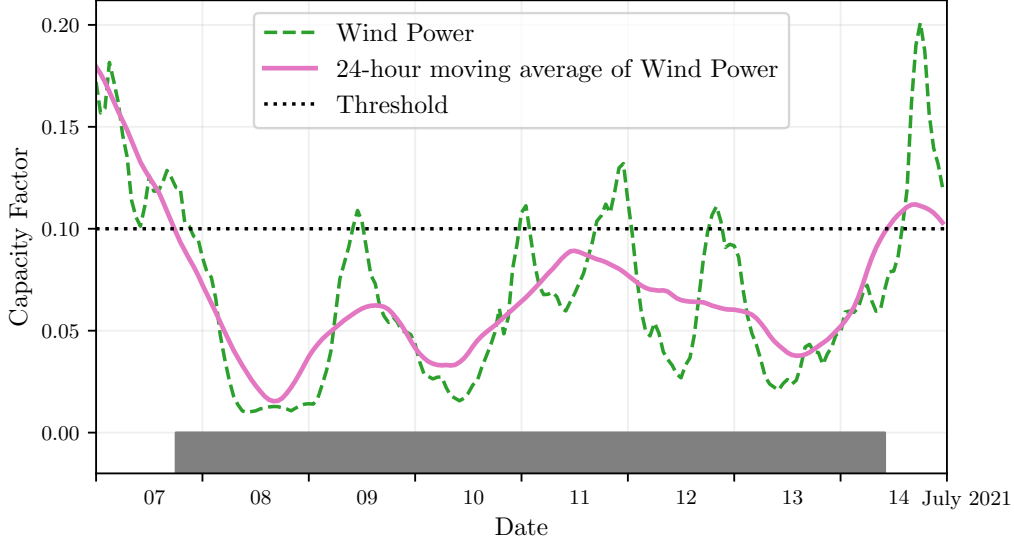


Figure 1: Wind time series of CF (green) and its 24-hour moving average (pink) from the 7th to the 15th of July 2021. The black dashed line indicates the CF threshold. The grey bar shows the period identified as a wind drought under our definition

4. Results

4.1. Verification

The accuracy of the datasets used in this study was verified, before continuing to the analysis of RES droughts. For the verification process, time-varying values of installed capacity were used to account for changes in RES development over the verification period. This step allowed us to assess how well the datasets represent the production of renewable energy by comparing them against observed data.

4.1.1. Wind Energy

The C3S datasets use the Vestas V136/3450 wind turbine power curve (Fig. 2a). The Atlite model allows the user to specify the power curve. We considered the 121 power curves available for download from Renewables.ninja [22]. For each power curve, Renewables.ninja also provides four associated smoothed power curves. The smoothing is done using a Gaussian filter with different standard deviations that depend on the wind speed. A separate wind CF time series for Ireland was generated for each of the wind turbine power curves and smoothing levels.

264 The performance of each CF time series is then assessed based on four skill
 265 scores: correlation coefficient (CC), root mean square error (RMSE), mean
 266 bias error (MBE), and the percentage of overlap. The percentage of overlap
 267 quantifies the similarity between the observed and modelled distributions. It
 268 is a positively oriented skill score, where 100% shows full agreement between
 269 the two distributions, and 0% indicates no overlap. The histograms of hourly
 270 CF values for the most recent decade (2014-2023) are used to calculate this
 271 skill score.

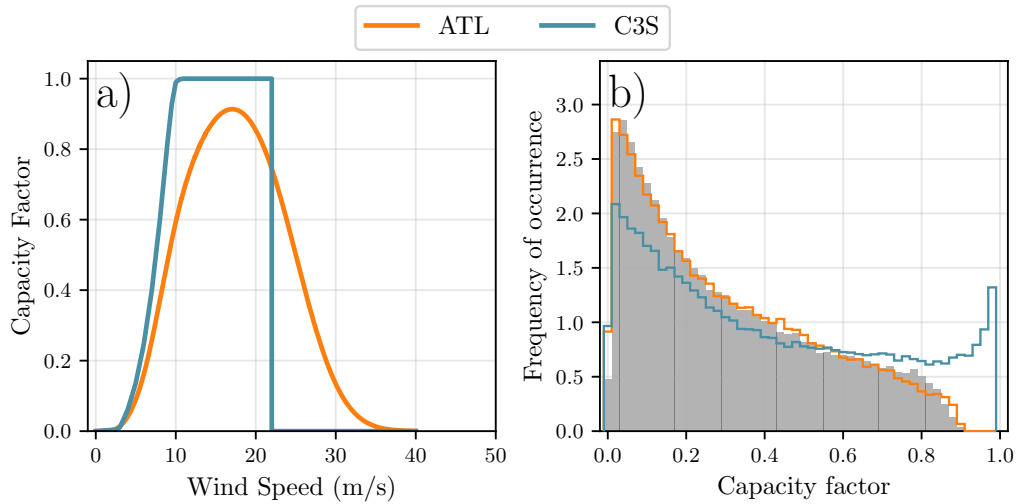


Figure 2: a) Power curves of the Enercon E112.4500 with a $0.3w$ smoothing filter used by ATL (orange) and the Vestas V136/3450 used by C3SE (blue) b) Histograms of wind CF for Ireland from ATL (orange), C3SE (blue) and Observed (shaded)

272 Based on these metrics, the most representative power curve for Ireland
 273 is the Enercon E112.4500 power curve with the $0.3w$ smoothing filter. The
 274 smoothing of the wind turbine power curve represents losses associated with
 275 each turbine, as well as losses such as wake effects between turbines, which
 276 are important when modelling wind energy on larger spatial scales. The
 277 histogram in Fig. 2b shows that the C3SE power curve tends to underestimate
 278 low CF values and overestimate higher ones, whereas the smoothed ATL
 279 power curve more closely follows the observed wind availability data. This
 280 is further supported by the percentage of overlap which is higher for ATL
 281 (97.2%) than for C3SE (83.2%), indicating better agreement with observed
 282 data.

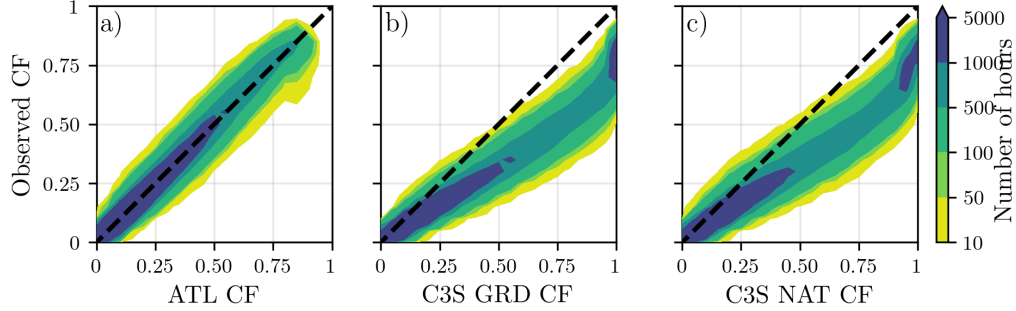


Figure 3: Wind CF density plot of the observed CF (vertical axes) and modelled (horizontal axes) CF data for the a) ATL, b) C3S GRD and c) C3S NAT datasets

283 The effect of the difference between the power curves is also visible in
 284 Fig. 3, which shows a density plot of wind CF values. The two C3S datasets
 285 are shown to overestimate the observed CF, whereas the ATL dataset is in
 286 good agreement with the observed data. The skill scores presented in Table 2
 287 show that ATL performs better than the two C3S datasets for all of the skill
 288 scores.

	ATL	C3S GRD	C3S NAT
CC	0.981	0.972	0.970
RMSE	0.045	0.177	0.162
MBE	-0.003	0.137	0.121

Table 2: Skill scores for wind power for the three datasets compared to observed data

289 Fig. 4 shows the average annual number of wind drought events during
 290 the 2014 to 2023 validation period. The figure reveals that ATL presents
 291 the best overall agreement with the observed frequency and duration of wind
 292 drought events. This pattern is particularly evident for shorter-duration
 293 events, which are the most frequent.

294 This verification for wind generation data highlights the importance of
 295 selecting a representative wind turbine power curve for the region being anal-
 296 ysed. The ATL dataset, which uses a representative wind turbine power
 297 curve, is skilled at reproducing wind CF and droughts over Ireland. On the
 298 other hand, the power curve used for both C3S GRID and C3S NAT is not
 299 representative for Ireland, as it severely overestimates generation, underes-
 300 timating the occurrence of RES droughts. This highlights a problem with

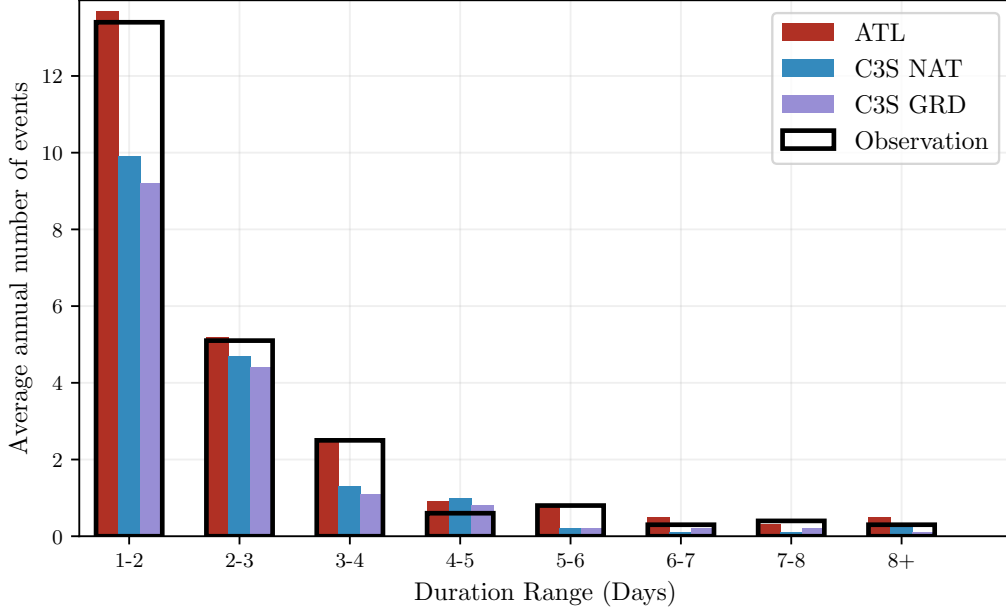


Figure 4: Average annual number of wind drought events for ATL (red), C3S GRD (blue), C3S NAT (purple), and the observed data (black outline). The wind droughts are identified from 2014 to 2023, considering the actual capacity of the system at any given time

301 using generalised datasets for analysing RES droughts: biases severely affect
302 their ability to accurately reproduce RES drought events. The skill scores
303 for the three datasets (Tab. 2) show only a small difference in their ability to
304 reproduce the changes in CF, as seen by their similar CC scores. However,
305 their ability to reproduce the actual CF values is much lower than that of
306 ATL, with RMSE scores almost four times bigger for the two C3S datasets.
307 There is a clear bias towards an overestimation of CF, seen in the MBE
308 values, which leads to the underestimation of droughts. This highlights the
309 need to use regionally verified models to assess RES droughts.

310 4.1.2. Solar PV Energy

311 The Atlite model allows the user to select certain PV panel characteristics.
312 In this study, the three PV panel types available in the Atlite model were
313 considered (CSi, CdTe, Kaneka). Following the same methodology as in the
314 previous section, the three available models were compared using four skill
315 scores (CC, RMSE, MBE, and the percentage of overlap). Based on the best-
316 performing metrics, the Beyer PV panel model was selected [25], using the

317 Kaneka Hybrid panel option. For all solar PV farm locations, the azimuth
318 angle is fixed at 180° (due south), and the optimal tilt angle option is applied.
319 The solar PV installed capacity available on the spreadsheets from Eir-
320 Grid represents the Maximum Export Capacity (MEC) and does not ac-
321 curately reflect the installed solar PV capacity. To enable actual solar PV
322 generation potential to be modelled correctly, installed capacities were set at
323 1.4 times the MEC values. This scaling factor was estimated by analysing
324 proprietary data from individual solar PV farms provided by EirGrid, which
325 showed that, on average, assuming that the installed capacities of farms ex-
326 ceed their MEC values by 40% yields the best agreement with the observed
327 availability.

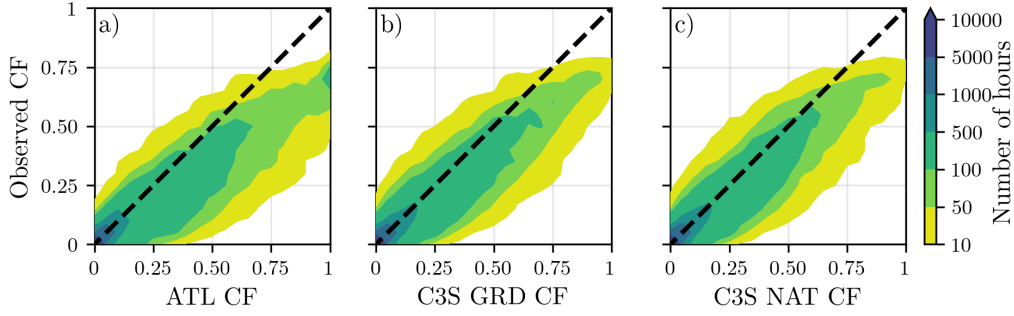


Figure 5: Solar PV CF density plot of the observed (vertical axes) and modelled (horizontal axes) CF series for the a) ATL, b) C3S GRD and c) C3S NAT datasets

328 Fig. 5 shows that the three datasets have a similar tendency to overesti-
329 mate the CF compared to the observed values, especially for high CF values.
330 The skill scores presented in Table 3 indicate that C3S GRD and C3S NAT
331 perform better than ATL for solar PV CF, with lower RMSE and MBE,
332 and higher CC scores. This may be due to the statistical approach taken by
333 C3SE for the orientation of the PV panels.

	ATL	C3S GRD	C3S NAT
CC	0.921	0.931	0.931
RMSE	0.119	0.090	0.113
MBE	0.046	0.027	0.021

Table 3: Skill scores for solar PV CF for the three datasets compared to observed data

334 Fig. 6 shows the number of solar PV drought events during the 2023

validation period across different duration ranges. The figure reveals partial agreement between the three datasets and the observed data, with consistent results noticed for duration ranges of 1-2, 3-4, 7-8, and 8+ days. However, discrepancies appear in the other ranges, where the models diverge from the observed data. The main challenge in validating solar PV data stems from the recent installation of a large share of Ireland’s solar PV capacity, with over 65% of the total solar PV capacity installed in 2023. This results in uncertainties in solar PV generation data and the actual generating capacity in the first few months after each farm is connected. Overall, C3S GRD performs slightly better than the other datasets in reproducing observed solar PV drought events.

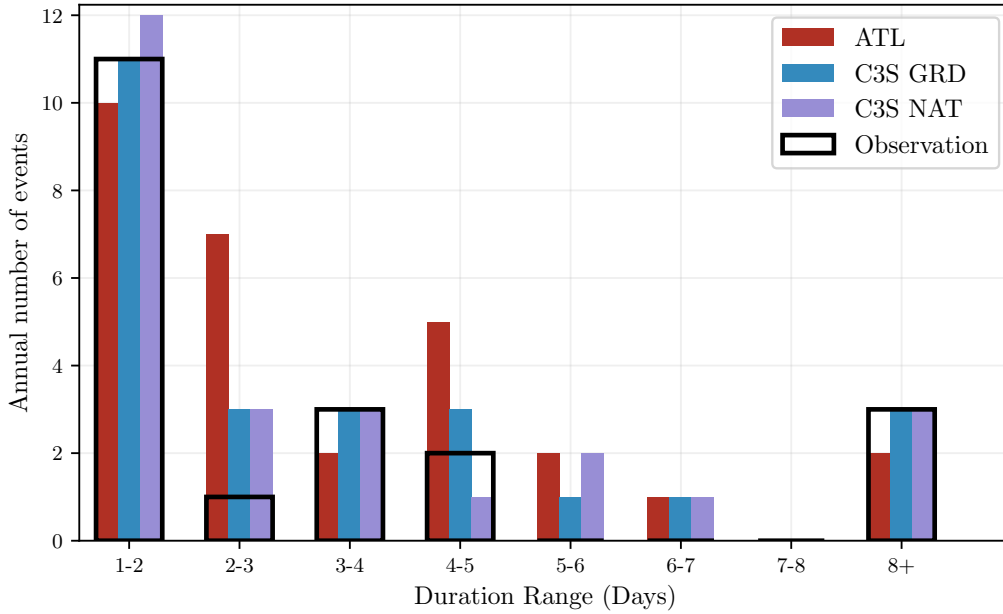


Figure 6: Number of solar PV drought events for ATL (red), C3S GRD (blue), and C3S NAT (purple) and the observed data (black outline). The solar PV droughts are identified for 2023, considering the actual capacity of the system at any given time

4.2. Analysis

In this section, RES droughts are analysed by calculating the frequency and duration of RES drought events, the return periods for different RES

349 drought durations, and the seasonality of RES drought events. Understand-
350 ing the characteristics and timing of RES drought events enables system op-
351 erators to optimally plan for reserve capacity requirements, ensuring grid sta-
352 bility and security of supply. Results are presented for the three datasets, al-
353 lowing their differences on the characterisation of RES droughts to be clearly
354 identified.

355 RES drought events are evaluated under two different scenarios with fixed
356 installed capacities: the 91W-9PV scenario, with 5.9 GW of wind capacity
357 and 0.6 GW of solar PV capacity; and the 57W-43PV scenario, where wind
358 capacity comprises 11.45 GW and solar PV capacity increases to 8.6 GW.
359 Both scenarios were driven by 45 years of ERA5 data. Using the RES drought
360 identification process described in Section 3.5, wind and solar PV droughts
361 are first analysed separately before presenting the results for combined (wind
362 + solar PV) RES droughts under both scenarios.

363 4.2.1. *Annual Number of RES Droughts*

364 The first part of the analysis examines the annual number of RES drought
365 events. When only wind energy is considered (Fig.7a), the number of drought
366 events decreases as the duration range increases, with very few events lasting
367 more than seven days. In contrast, for solar PV energy (Fig.7b), drought
368 frequency declines from one to eight days and then slightly increases for
369 longer durations. This behaviour is attributable to Ireland’s high-latitude
370 location, where reduced sunlight in winter (from November to March) leads
371 to consistently low solar PV output.

372 Moreover, the comparison between wind and solar PV results indicates
373 that the median, first, and third quartiles for solar PV are consistently higher
374 than or equal to those for wind. This is expected, given that solar PV gener-
375 ation is inherently lower, zero at night, and limited by the solar cycle. When
376 wind and solar PV are combined under the 91W-9PV scenario (Fig.7c), the
377 results closely mirror those of wind alone, due to the dominance of wind power
378 in the current energy mix. However, in the 57W-43PV scenario (Fig.7d), a
379 marked reduction in drought events is observed across all datasets, with a de-
380 crease of the total number of events of 56% for ATL, 52% for C3S GRD, and
381 50% for C3S NAT, demonstrating the beneficial effects of a more balanced
382 energy mix.

383 The consistently higher RES drought counts reported by the ATL dataset,
384 compared to the C3S datasets, underscore the importance of wind turbine
385 power curve representation when quantifying RES droughts. Whereas the

three datasets agree on the overall effect of balancing the share of wind and solar PV generation, they differ at a quantitative level, which has crucial implications for energy planning.

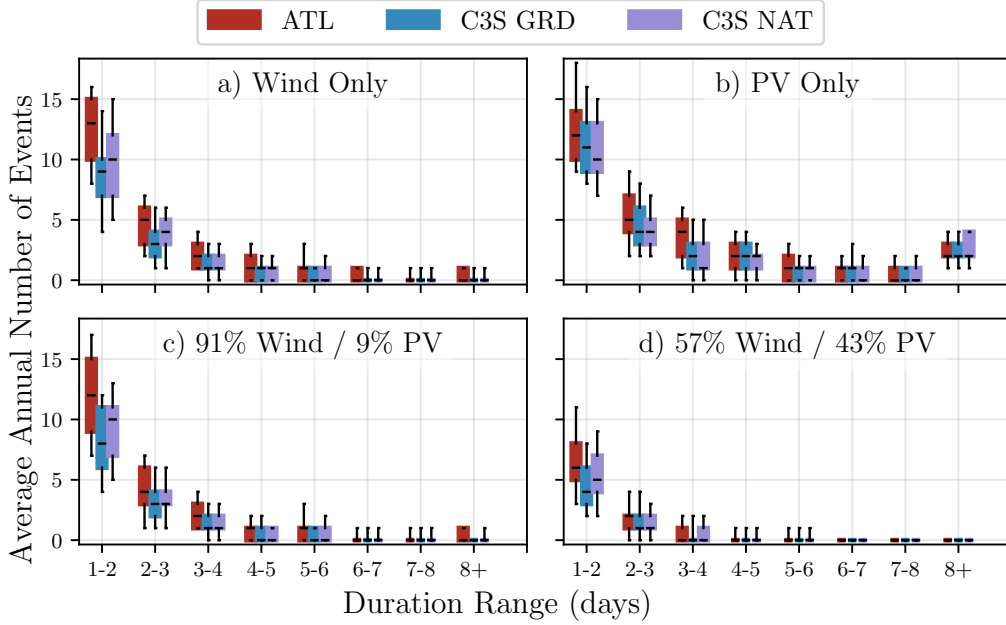


Figure 7: Average annual number of RES droughts (from 1979 to 2023) for a) Wind, b) solar PV, c) 91W-9PV and d) 57W-43PV for ATL (red), C3S GRD (blue), and C3S NAT (purple). The x-axis represents duration ranges in days (lower bound included), while the y-axis indicates the annual number of events. The boxes display the first and third quartiles and the median is marked by a black line. The whiskers indicate the 5th and 95th percentiles

4.2.2. Return Periods of RES Drought Duration

RES drought events identified over the 45-year period were used to calculate the return periods for different RES drought durations. A return period is the estimated average time interval between events of a specified duration (not to be confused with the frequency of their occurrence within a fixed time frame). Fig. 8 shows the return periods for different RES drought durations, which can be used to capture the most extreme events affecting the system. Understanding their return periods is crucial, as extreme yet rare RES droughts pose the toughest challenge to energy security by placing

398 significant strain on the conventional backup sources necessary to maintain
399 security of supply during these events.

400 The duration of wind droughts (Fig. 8a) increases in a log-linear fashion
401 across the three datasets. The log-linear trend indicates a predictable rela-
402 tionship between wind drought duration and occurrence, with longer wind
403 droughts becoming exponentially less likely as duration increases. In the case
404 of solar PV droughts (Fig. 8b), Atlite behaves differently than the two C3S
405 datasets. The ATL dataset show a generally log-linear increase. For C3S
406 GRD and C3S NAT, the duration of PV droughts increases in a log-linear
407 pattern for events lasting less than 16 days. Beyond this duration, there is
408 a sharp rise in solar PV drought duration for events up to a one-year return
409 period. This sudden increase again reflects the impact of extended periods of
410 low PV generation during winter in Ireland. The difference between the ATL
411 and the C3S results arises from differences in the datasets near the threshold
412 of 0.1 CF. ATL remains slightly above the threshold more frequently during
413 these conditions, leading to shorter, more fragmented RES drought events.
414 In contrast, C3S GRD and C3S NAT tend to fall below the threshold in simi-
415 lar conditions, resulting in longer continuous RES drought periods, especially
416 during winter.

417 Under the 91W-9PV scenario (Fig. 8c), the combined RES drought return
418 periods mirror those for wind alone, reflecting the dominance of wind in the
419 current energy mix. In contrast, the 57W-43PV scenario (Fig. 8d) shows
420 a dramatic increase in return periods across all durations, suggesting that
421 a more diversified energy mix can substantially mitigate the frequency of
422 prolonged RES drought events. For example, the return period for a five-day
423 RES drought event (shown by the vertical dashed lines in Fig. 8) extends
424 from roughly six months for the 91W-9PV scenario, to four years for the
425 57W-43PV scenario in the ATL dataset, and from about fifteen months to
426 around five years in the two C3S datasets. Despite the lower wind share in the
427 57W-43PV scenario, typically known for its relative stability, the balanced
428 share with solar PV leads to extended return periods for RES droughts. This
429 result indicates that the complementarity between wind and solar PV plays a
430 crucial role in reducing the occurrence of RES drought events in a diversified
431 energy portfolio.

432 Across Fig. 8a, c, and, d, the return periods in the ATL dataset are con-
433 sistently higher than those in the two C3S datasets. For instance, in the
434 91W-9PV scenario (Fig. 8c), an event with a one-year return period lasts six
435 days in the ATL dataset, compared to only five days in the C3S datasets.

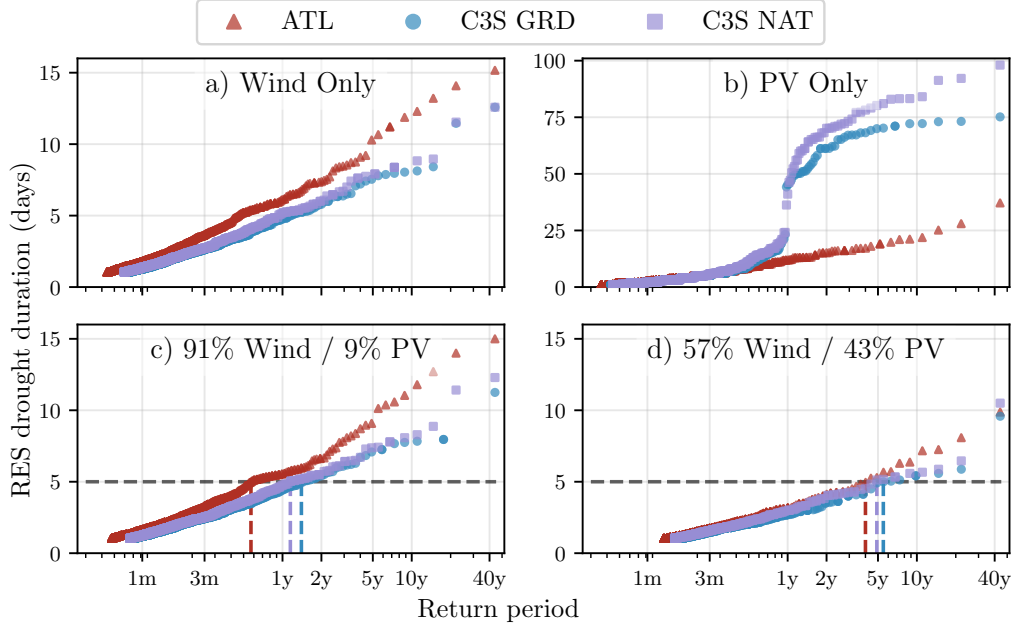


Figure 8: Return periods of the duration of RES droughts (from 1979 to 2023) for a) Wind, b) Solar PV, c) 91W-9PV and d) 57W-43PV for ATL (red triangle), C3S GRD (blue circle), and C3S NAT (purple square). The x-axis represents the return period time in a log-scale and the y-axis indicates the duration of RES drought associated with it. The horizontal dashed line marks the 5-day return period, with coloured vertical dashed marking its return period for each dataset

This difference underscores the importance of model selection when quantifying RES droughts, as each dataset's assumptions and parametrisations significantly influence RES droughts duration estimates. Additionally, in all four graphs, the similarity between results from the two C3S datasets suggests that assumptions in the ATL dataset, such as wind turbine power curve selection and PV panel specifications, have a greater impact on RES drought duration estimates than the precise geographic distribution of RES farms when studying the return periods of RES droughts.

The return periods calculated from the three datasets show large differences, in particular for the more extreme events with longer return periods. The C3S datasets produce shorter RES drought durations for these events, which would have the largest impact on the power system. This shows that system planning based on the wrong datasets could yield an underestimation

449 of the duration of extreme RES droughts, potentially leading to shortages
450 linked to undersized reserve capacity.

451 *4.2.3. Seasonal Distribution of RES Droughts*

452 The seasonal analysis of RES droughts is based on the percentage of hours
453 in each month classified as part of a RES drought event. Wind droughts tend
454 to be more frequent during summer, whereas solar PV droughts are more
455 common in winter due to reduced sunlight. By comparing these seasonal
456 patterns across different datasets and energy scenarios, this study examines
457 how model-specific assumptions and variations in capacity mix affect the
458 overall characterisation of RES drought events.

459 For the wind-only scenario (Fig. 9a), the ATL dataset exhibits a pro-
460 nounced seasonal pattern, with about 24% of summer hours (June, July,
461 August) identified as RES droughts compared to only 4% in winter (Decem-
462 ber, January, February). This strong seasonal signal is less evident in the C3S
463 datasets, which suggests that the differences in the underlying wind power
464 curves play a significant role. In ATL, CF near or below the 0.1 threshold
465 occurs at relatively higher wind speeds, resulting in a higher count of RES
466 drought hours during the summer months. In contrast, solar PV droughts
467 (Fig. 9b) display an opposite seasonal trend. Across all datasets, over 60%
468 of winter hours are classified as solar PV droughts, reflecting the naturally
469 low solar irradiance in Ireland during winter.

470 ATL tends to record a slightly higher percentage of RES drought hours
471 for wind and a marginally lower percentage for solar PV relative to the C3S
472 datasets. These differences highlight how dataset-specific assumptions, such
473 as the treatment of wind turbine power curves and PV panel characteristics,
474 significantly influences the apparent seasonal dynamics of RES droughts.

475 The 91W-9PV scenario (Fig. 9c) shows patterns comparable to the ones
476 for wind droughts (Fig. 9a). However, in the 91W/9PV scenario, the number
477 of hours classified as RES droughts in summer decreases slightly compared
478 to the wind-only scenario. This reduction can be explained by the contri-
479 bution of solar PV generation during the summer months in the 91W-9PV
480 scenario, even though it constitutes only 11% of total capacity. Since the
481 number of RES drought hours for solar PV in summer is near zero, this
482 small contribution has a noticeable impact on reducing overall RES drought
483 hours. In the 57W-43PV scenario (Fig. 9d), all three datasets show a re-
484 duction in monthly RES drought frequency. Annual reductions in median
485 RES drought frequency are observed across the datasets, dropping from 14%

486 to 5% for ATL, from 8% to 3% for C3S GRD, and from 9% to 4% for C3S
 487 NAT. The balanced mix of wind and solar PV power in this scenario reduces
 488 the seasonal signal overall and significantly decreases the percentage of RES
 489 drought hours in the summer.

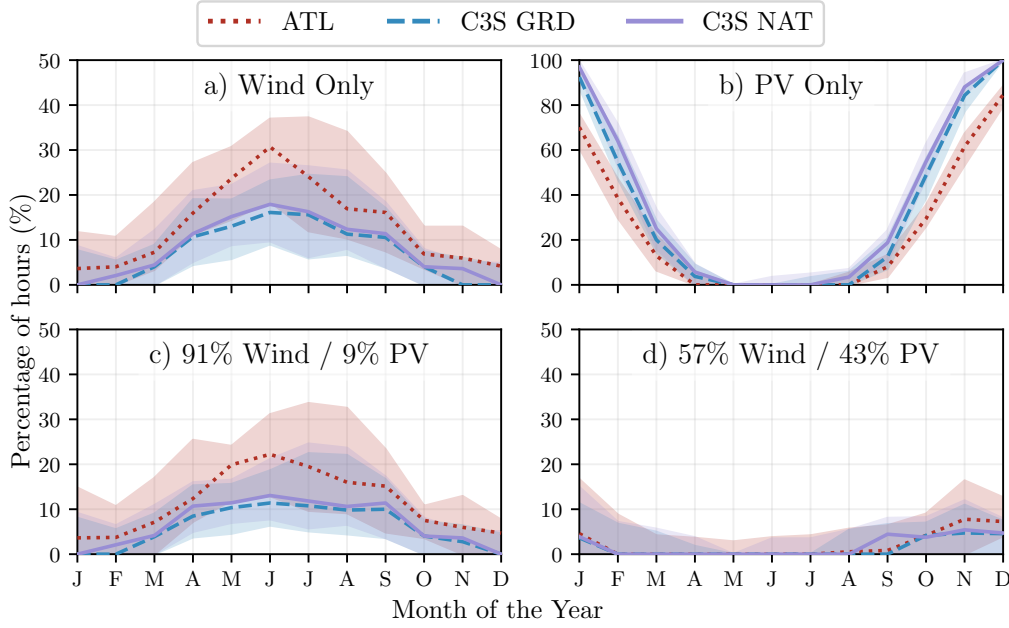


Figure 9: Percentage of hours in a month which are part of a RES drought (from 1979 to 2023) for a) Wind, b) Solar PV, c) 91W-9PV and d) 57W-43PV for ATL (red dotted), C3S GRD (blue dashed), and C3S NAT (purple solid). The x-axis represents the month of the year, and the y-axis indicates the percentage of hours. Lines correspond to the median values and the area between the first and third quartiles is shaded. Note the different y-axis scale for b).

490 The seasonal variations of RES droughts observed in this study have im-
 491 portant implications for energy planning. Energy demand peaks in winter
 492 for Northern European countries, making the seasonality of RES droughts
 493 critical for the sizing of reserve capacity. Our results show that selecting
 494 the wrong dataset could severely underestimate RES droughts during winter
 495 months, thereby affecting the reliability of the energy system during critical
 496 periods. Additionally, the integration of large shares of solar PV in the system
 497 leads to a generalised reduction of RES droughts, yet winter months present
 498 a slight increase. The natural limitations of solar PV lead to inevitably

499 higher reserve capacity needs during winter months as reliance on RES in-
500 creases. These types of insights are essential to develop targeted strategies
501 that enhance grid resilience and ensure a stable energy supply throughout
502 the year.

503 5. Conclusions

504 This study has explored the characterisation of RES droughts in the real-
505 life transition from a wind-dominated system to a more balanced system
506 with integrated solar PV. This has been done through the comparison over
507 a 45-year period of three different datasets: one based on a hand-crafted
508 validated model and two based on a generic model, C3S-Energy. The generic
509 model has two versions, one using large-scale aggregated information, and
510 one which includes the locations of farms as well (also considered in the
511 validated model).

512 Our results show that generic datasets present limitations in the quan-
513 tification of RES droughts. Although the three datasets used capture overall
514 trends in drought occurrence, significant differences emerge when using non-
515 tailored data for the study of RES droughts. This finding highlights that the
516 choice of dataset and its underlying assumptions can lead to consequential
517 differences in estimated RES drought characteristics, emphasising the need
518 for datasets that are specifically designed for extreme event analysis.

519 This study reveals that differences in model parametrisation, particu-
520 larly in the representation of wind turbine power curves and solar PV panel
521 characteristics, have a stronger influence on the drought estimates than the
522 inclusion of RES farm locations. The use of a validated dataset with a care-
523 fully selected wind turbine power curve consistently produced higher return
524 periods and a greater number of drought events for wind energy than the
525 datasets derived from C3S-Energy. This suggests that fine-tuning model pa-
526 rameters to match observed data is crucial for accurately quantifying RES
527 drought risks, thereby supporting more effective energy system planning.

528 Finally, the effect on RES droughts of the integration of solar PV in
529 a wind-dominated system has been explored in a real-case setting. In the
530 presented example of Ireland, the analysis has demonstrated that transition-
531 ing to a more balanced system with similar amounts of wind and solar PV
532 markedly reduces the frequency, duration, and seasonal variability of drought
533 events. This improvement is attributed to the complementary nature of wind
534 and solar PV generation, as solar PV typically peaks in summer while wind

535 generation is more consistent in winter. Thus, a more diversified renewable
536 energy mix not only mitigates extreme drought conditions but also enhances
537 overall system resilience, providing valuable insights for policymakers tasked
538 with ensuring energy security.

539 The results presented in this study have several limitations. Although
540 ERA5 is among the best reanalysis datasets for renewable energy analysis,
541 it still presents some biases, and its resolution may not capture local-scale
542 phenomena. This is especially limiting if individual farms are considered, but
543 its still shows good skill at statistically representing nation-wide behaviours
544 considering the distribution of farms. Moreover, the methodology employs a
545 fixed threshold to define RES drought events, which is necessary for compar-
546 ing the three datasets considering only weather-derived drivers, but does not
547 account for demand variations. Consequently, while this approach enables a
548 consistent inter-comparison, it will not signal events that are most critical for
549 power system operations for their mismatch of RES generation and demand.

550 Future work is planned to extend the current analysis. First, climate pro-
551 jection data will be integrated with different energy scenarios, incorporating
552 the addition of offshore wind, to better understand how climate change might
553 affect RES droughts. Second, expanding the geographic domain of the study
554 to include the rest of Europe would provide a more comprehensive under-
555 standing of RES droughts in an interconnected electricity grid. This would
556 require extensive verification across other European countries, making it a
557 more complex but highly relevant challenge.

558 Data Availability

559 The ERA5 data can be obtained from the Climate Data Store (<https://doi.org/10.24381/cds.adbb2d47>). The C3SE dataset is also available
560 from the Climate Data Store (<https://doi.org/10.24381/cds.4bd77450>).
561 Information on wind and solar PV farms in Ireland can be obtained from
562 the EirGrid website (<https://www.eirgrid.ie/grid/system-and-renewable-data-reports>). The Atlite model used in this study is open-source
563 and can be found on GitHub (<https://github.com/pypsa/atlite>). The
564 data and code required to reproduce the analysis in this article will be made
565 available upon acceptance of the manuscript in a public GitHub repository.
567

568 Acknowledgments

569 The research conducted in this publication was funded by Science Foun-
570 dation Ireland and co-funding partners under grant number 21/SPP/3756
571 through the NexSys Strategic Partnership Programme.

572 References

- 573 [1] EuroStat, Renewable Energy Statistics, 2023. URL: https://ec.europa.eu/eurostat/statistics-explained/index.php?title=Renewable_energy_statistics, Accessed: 2024-11-06.
- 574
575
- 576 [2] H. C. Bloomfield, D. J. Brayshaw, L. C. Shaffrey, P. J. Coker, H. E. Thornton, Quantifying the increasing sensitivity of power systems to climate variability, *Environmental Research Letters* 11 (2016) 124025. doi:10.1088/1748-9326/11/12/124025.
- 577
578
579
- 580 [3] H. C. Bloomfield, D. J. Brayshaw, A. Troccoli, C. M. Goodess, M. De Felice, L. Dubus, P. E. Bett, Y.-M. Saint-Drenan, Quantifying the sensitivity of european power systems to energy scenarios and climate change projections, *Renewable Energy* 164 (2021) 1062–1075. doi:10.1016/j.renene.2020.09.125.
- 581
582
583
584
- 585 [4] F. Kaspar, M. Borsche, U. Pfeifroth, J. Trentmann, J. Drücke, P. Becker, A climatological assessment of balancing effects and shortfall risks of photovoltaics and wind energy in germany and europe, *Advances in Science and Research* 16 (2019) 119–128. doi:10.5194/asr-16-119-2019.
- 586
587
588
589
- 590 [5] F. Mockert, C. M. Grams, T. Brown, F. Neumann, Meteorological conditions during periods of low wind speed and insolation in Germany: The role of weather regimes, *Meteorological Applications* 30 (2023) e2141. doi:10.1002/met.2141.
- 591
592
593
- 594 [6] M. Ohba, Y. Kanno, D. Nohara, Climatology of dark doldrums in japan, *Renewable and Sustainable Energy Reviews* 155 (2022) 111927. doi:10.1016/j.rser.2021.111927.
- 595
596
- 597 [7] M. J. Mayer, B. Biró, B. Szücs, A. Aszódi, Probabilistic modeling of future electricity systems with high renewable energy penetration using
- 598

- 599 machine learning, *Applied Energy* 336 (2023) 120801. doi:10.1016/j.
600 apenergy.2023.120801.
- 601 [8] D. Raynaud, B. Hingray, B. François, J. Creutin, Energy droughts from
602 variable renewable energy sources in European climates, *Renewable*
603 *Energy* 125 (2018) 578–589. doi:https://doi.org/10.1016/j.renene
604 .2018.02.130.
- 605 [9] A. Gangopadhyay, A. K. Seshadri, N. J. Sparks, R. Toumi, The role
606 of wind-solar hybrid plants in mitigating renewable energy-droughts,
607 *Renewable Energy* 194 (2022) 926–937. doi:10.1016/j.renene.2022.
608 05.122.
- 609 [10] J. Kapica, J. Jurasz, F. A. Canales, H. Bloomfield, M. Guezgouz,
610 M. De Felice, Z. Kobus, The potential impact of climate change on
611 european renewable energy droughts, *Renewable and Sustainable En-*
612 *ergy Reviews* 189 (2024) 114011. doi:10.1016/j.rser.2023.114011.
- 613 [11] K. Z. Rinaldi, J. A. Dowling, T. H. Ruggles, K. Caldeira, N. S. Lewis,
614 Wind and Solar Resource Droughts in California Highlight the Benefits
615 of Long-Term Storage and Integration with the Western Interconnect,
616 *Environmental Science and Technology* 55 (2021) 6214–6226. doi:10.1
617 021/acs.est.0c07848.
- 618 [12] P. T. Brown, D. J. Farnham, K. Caldeira, Meteorology and climatology
619 of historical weekly wind and solar power resource droughts over western
620 North America in ERA5, *SN Applied Sciences* 3 (2021) 814. doi:10.1
621 007/s42452-021-04794-z.
- 622 [13] S. Allen, N. Otero, Standardised indices to monitor energy droughts,
623 *Renewable Energy* 217 (2023) 119206. doi:10.1016/j.renene.2023.11
624 9206.
- 625 [14] C. Bracken, N. Voisin, C. D. Burleyson, A. M. Campbell, Z. J. Hou,
626 D. Broman, Standardized benchmark of historical compound wind and
627 solar energy droughts across the Continental United States, *Renewable*
628 *Energy* 220 (2024) 119550. doi:https://doi.org/10.1016/j.renene
629 .2023.119550.
- 630 [15] H. Lei, P. Liu, Q. Cheng, H. Xu, W. Liu, Y. Zheng, X. Chen, Y. Zhou,
631 Frequency, duration, severity of energy drought and its propagation in

- hydro-wind-photovoltaic complementary systems, *Renewable Energy* (2024) 120845. doi:10.1016/j.renene.2024.120845, 2.
- [16] H. Hersbach, B. Bell, P. Berrisford, S. Hirahara, A. Horányi, J. Muñoz-Sabater, J. Nicolas, C. Peubey, R. Radu, D. Schepers, et al., The ERA5 global reanalysis, *Quarterly Journal of the Royal Meteorological Society* 146 (2020) 1999–2049. doi:10.1002/qj.3803.
- [17] L. Dubus, Y. Saint-Drenan, A. Troccoli, M. De Felice, Y. Moreau, L. Ho-Tran, C. Goodess, R. Amaro E Silva, L. Sanger, C3S Energy: A climate service for the provision of power supply and demand indicators for Europe based on the ERA5 reanalysis and ENTSO-E data, *Meteorological Applications* 30 (2023) e2145. doi:10.1002/met.2145.
- [18] F. Hofmann, J. Hampp, F. Neumann, T. Brown, J. Hörsch, Atlite: a lightweight Python package for calculating renewable power potentials and time series, *Journal of Open Source Software* 6 (2021) 3294. doi:10.21105/joss.03294.
- [19] A. Kies, B. U. Schyska, M. Bilousova, O. El Sayed, J. Jurasz, H. Stoecker, Critical review of renewable generation datasets and their implications for european power system models, *Renewable and Sustainable Energy Reviews* 152 (2021) 111614. doi:10.1016/j.rser.2021.111614.
- [20] EirGrid & SONI, System and Renewable Data Reports, 2023. URL: <https://www.eirgrid.ie/grid/system-and-renewable-data-reports>, Accessed: 2024-11-06.
- [21] Y.-M. Saint-Drenan, L. Wald, T. Ranchin, L. Dubus, A. Troccoli, An approach for the estimation of the aggregated photovoltaic power generated in several European countries from meteorological data, *Advances in Science and Research* 15 (2018) 51–62. doi:10.5194/asr-15-51-2018.
- [22] I. Staffell, S. Pfenninger, Using bias-corrected reanalysis to simulate current and future wind power output, *Energy* 114 (2016) 1224–1239. doi:10.1016/j.energy.2016.08.068.
- [23] Government of Ireland, Climate Action Plan 2024, Technical Report 3, Department of the Environment, Climate and Communications, 2023.

- 665 URL: [https://www.gov.ie/pdf/?file=https://assets.gov.ie/](https://www.gov.ie/pdf/?file=https://assets.gov.ie/284675/70922dc5-1480-4c2e-830e-295afd0b5356.pdf)
666 [284675/70922dc5-1480-4c2e-830e-295afd0b5356.pdf](https://www.gov.ie/pdf/?file=https://assets.gov.ie/284675/70922dc5-1480-4c2e-830e-295afd0b5356.pdf), Accessed:
667 2024-11-06.
- 668 [24] Sustainable Energy Authority Ireland, National Energy Projections
669 2024, Technical Report, Sustainability Energy Authority of Ireland,
670 2024. URL: [https://www.seai.ie/news-and-events/news/energ](https://www.seai.ie/news-and-events/news/energy-projections-report)
671 [y-projections-report](https://www.seai.ie/news-and-events/news/energy-projections-report), Accessed: 2024-11-06.
- 672 [25] H. G. Beyer, G. Heilscher, S. Bofinger, A robust model for the mpp
673 performance of different types of pv-modules applied for the performance
674 check of grid connected systems, Eurosun (2004) 8.